Numerical Methods in Civil Engineering, 10-3 (2026) 61-79

Numerical Methods in Civil Engineering

Journal Homepage: https://nmce.kntu.ac.ir/

Analytical-numerical study of coupled shear panels with easy-yielding steel plates under the lateral loadings

Soroush Mosayyebi*, Niloofar Moniri*, Saeid Sabouri-Ghomi**

ARTICLE INFO

RESEARCH PAPER

Article history:
Received:
December 2025
Revised:
February 2026
Accepted:
May 2026

Keywords:

Shear Panels,
Easy-Yielding Steel Plate,
Nonlinear Static Analysis,
Analytical Relationships,
Numerical Verification

Abstract:

In this study, the structural behavior of coupled shear panels with Easy-Yielding steel plates is thoroughly investigated. These advanced systems are designed to enhance energy dissipation while ensuring a controlled and predictable yielding mechanism in seismic-resistant structures. To this end, after introducing the design assumptions, three one-story, prototype-scale numerical models with Shear, Intermediate and Flexural link beam behaviors are designed using the Plate-Frame Interaction method, and the corresponding analytical formulations are derived. The selected configurations effectively capture diverse force transfer and deformation mechanisms typically encountered in practical engineering structures. Subsequently, the specimens are modeled in Abaqus software and subjected to nonlinear static analysis to verify the yielding sequence of structural members and evaluate the overall nonlinear response. Pushover curves are extracted afterwards and systematically analyzed to assess strength capacity and overall deformation characteristics. The results demonstrate that the proposed analytical formulations are fully consistent with the numerical simulations performed in Abaqus, as both approaches predict the same yielding sequence of structural members, which is a primary objective of the design.

1. Introduction

The Coupled Steel Plate Shear Wall (C-SPSW) is an innovative configuration of the conventional steel plate shear wall system, in which the shear panels at the story levels are interconnected through Coupling Beams (CBs). A schematic view of a typical coupled steel plate shear wall is presented in Figure 1. In this study, the investigation focuses on a single story of the coupled steel plate shear wall system, extracted from the overall structure as shown in Figure 1. From a structural behavior standpoint, this story effectively represents a "coupled shear panel". Each shear panel, as illustrated in Figure 1, consists of a steel web plate that is bounded by an External Vertical Boundary Element (EVBE), an Internal Vertical Boundary Element (IVBE), and a Horizontal Boundary Element (HBE).

* *Department of Civil Engineering, K. N. Toosi University of Technology, Tehran 1996715433, Iran.*
** *Corresponding author: Professor, Department of Civil Engineering, K. N. Toosi University of Technology, Tehran 1996715433, Iran. Email: sabouri@kntu.ac.ir*

Previous research has shown that this system exhibits excellent structural performance in terms of stiffness, strength, ductility, energy dissipation, and related parameters. In addition, due to the incorporation of openings, this system is also highly efficient architecturally. Furthermore, studies indicate that the application of this structural system is economically advantageous. It should be noted that, since the use of this system has only been introduced over the past two decades, it is considered a relatively new topic with substantial potential for further research and development.

In this study, the web plates are made of Easy-Yielding steel. The use of Easy-Yielding steel plates offers numerous advantages, several of which are discussed below. For brevity, these steels are hereafter referred to by the abbreviation **EYS**.

Although previous studies have investigated the behavior and design of coupled steel plate shear walls and the use of EYS, limited attention has been given to the application of

https://doi.org/10.61882/NMCE.2512.1118

EYS in such systems. In particular, the performance ranges of coupling beams constructed with EYS, considering shear, flexural, and combined mechanisms under the Plate–Frame Interaction (PFI) method, have not been systematically evaluated. Moreover, the impact of EYS on energy dissipation, story shear displacement, and critical stress thresholds in coupled shear panels remains insufficiently understood. Therefore, a clear need exists for a comprehensive analytical–numerical investigation to address these gaps and to provide practical design guidance for EYS-based coupled steel plate shear walls.

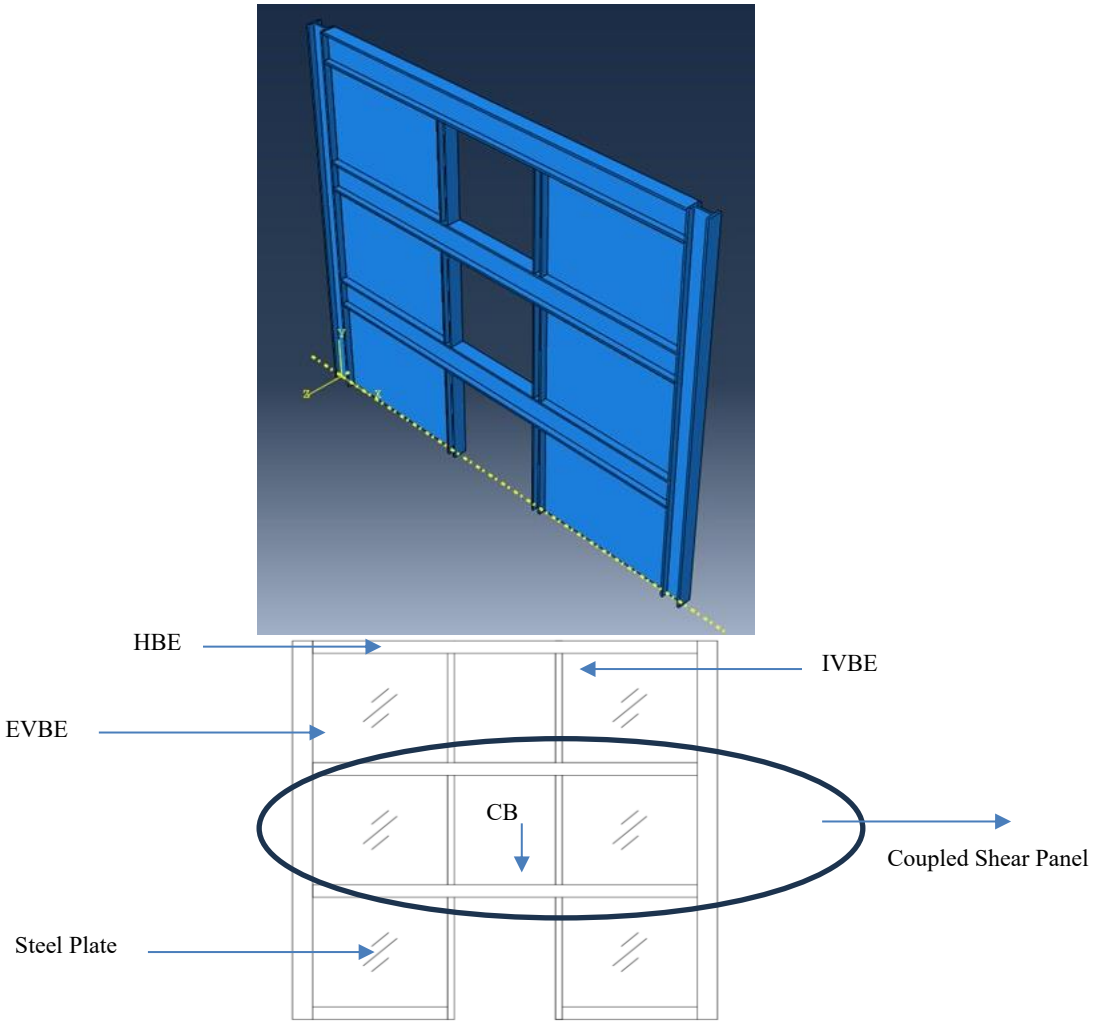

Fig. 1:3D (up) and 2D (down) Schematic Views of a Coupled Steel Plate Shear Wall (C-SPSW) and Coupled Shear Panel

In this study, the advantages of the EYS steel employed in the research are first introduced. Subsequently, the fundamental assumptions and the design procedure of the investigated specimens are presented based on the Plate–Frame Interaction (PFI) method. The applicable performance ranges corresponding to the shear, flexural, and combined behavioral mechanisms of the coupling beams (CBs) are then determined. Finally, comprehensive numerical simulations are carried out using Abaqus, and the results demonstrates an excellent agreement with the analytical relationships derived in the specimen design phase.

2. Literature Review

The initial idea of using coupled shear walls was proposed by Astaneh-Asl and Zhao [3], who examined the behavior of composite coupled shear walls under cyclic loading. Their study highlighted that coupled shear walls could effectively enhance ductility and energy dissipation under cyclic loads. Park and Yun studied the seismic behavior and the design of steel coupling beams [4]. They found that proper design of coupling beams significantly improves the overall lateral stiffness and energy absorption of the system. Fahnestock and Borello investigated the behavior and mechanisms of coupled steel plate shear walls [5]. Their work demonstrated that coupling panels contribute to more uniform load distribution and delay local buckling of web plates.
Abdollahzadeh and Malekzadeh studied the response modification factor of this system [6]. They concluded that the presence of coupling beams allows for higher response modification factors, enhancing seismic resilience. Ahn et al. conducted large-scale tests on coupled steel plate shear walls equipped with dampers [7]. The tests showed that damping devices in CBs could reduce peak inter-story drifts and improve hysteretic behavior. Borello et al. assessed the

feasibility of using coupled steel plate shear walls in high-seismic regions [8]. They found that this system performs reliably under strong seismic excitations, making it suitable for high-seismic zones.

Eshkvari et al. proposed an optimal design procedure for coupling panels in steel plate shear walls [9]. Their method ensures that both shear and flexural behaviors of coupling beams are properly controlled. Shekasteband and Pavir studied the hysteresis behavior of coupled steel plate shear walls [10]. They reported that energy dissipation capacity increases with proper detailing of boundary elements. Safari Gorji and Cheng investigated plastic design and performance-based design of coupled steel plate shear walls [11]. They highlighted that performance-based design can more accurately predict inelastic behavior and prevent premature failure.

Shayanfar et al. analyzed coupled steel plate shear walls with braced arms for tall buildings [12]. They observed that braced arms improve lateral stiffness and reduce story drifts for tall structures. Usefvand et al. studied the damage index of coupled steel plate shear wall systems under seismic loading [13]. They proposed damage indices that effectively quantify structural deterioration during seismic events. Wang et al. examined the damage indices and fragility assessment of coupled steel plate shear walls made of EYS [14]. Their results indicated that LYP steel plates enhance ductility and improve fragility characteristics compared to conventional steels.

Recent advances between 2021 and 2025 have focused on improving the seismic behavior and design of shear wall systems. Hao et al. (2023) demonstrated that incorporating slits in coupled steel plate shear walls enhances stiffness, lateral strength, and energy dissipation under cyclic loading [15]. Zirakian (2024) showed that seismic retrofitting of SPSWs using EYS significantly improves pushover and fragility responses [16]. Seismic performance evaluation of hybrid coupled shear walls with shear and flexural fuse-type coupling beams highlighted the dependence of energy dissipation and drift behavior on building scale and fuse configuration [17]. Experimental studies on hybrid coupled walls with replaceable LYP steel shear panel dampers reported enhanced seismic resilience and replaceability with advanced connections [18].

Pehlivan et al. (2025) found that cold-formed multi-panel shear walls provide increased ductility and load capacity under seismic actions [19]. Alhunami et al. (2025) confirmed that optimized coupled shear wall parameters reduce dynamic displacements [20]. In prefabricated shear wall constructions, the quality of coupling beam connections is crucial for overall seismic performance [21]. Lead viscoelastic coupling beams were found to enhance energy dissipation and reduce damage indices in coupled systems [22]. Modeling studies using OpenSees indicated that reinforcement and axial load ratios substantially influence ductility and seismic load capacity of grid shear walls [23]. Experimental investigations on novel composite RC shear walls with CFST frames exhibited superior seismic performance under cyclic loading [24].

This study focuses on an analytical–numerical investigation of coupled steel plate shear walls constructed with EYS plates. In the present paper, the design of the specimen using the Frame–Plate Interaction Method [1] and the derivation of the necessary analytical formulations are presented. Then the designed models were simulated in the *Abaqus* software to validate the extracted formulations, under nonlinear static analysis.

3. Easy-Yielding Steel (EYS)

In this section, the advantages of using EYS are presented through mathematical formulations. EYS is characterized by yield stresses below the typical range for conventional structural steels, generally between 90 and 110 MPa, while maintaining the same elastic modulus. Figure 2 illustrates a comparison of the shear displacement versus lateral load curves for EYS and conventional structural steels. [2] As illustrated in Figure 2, EYS steels undergo larger lateral displacements under the same ultimate lateral load, demonstrating superior ductile behavior.

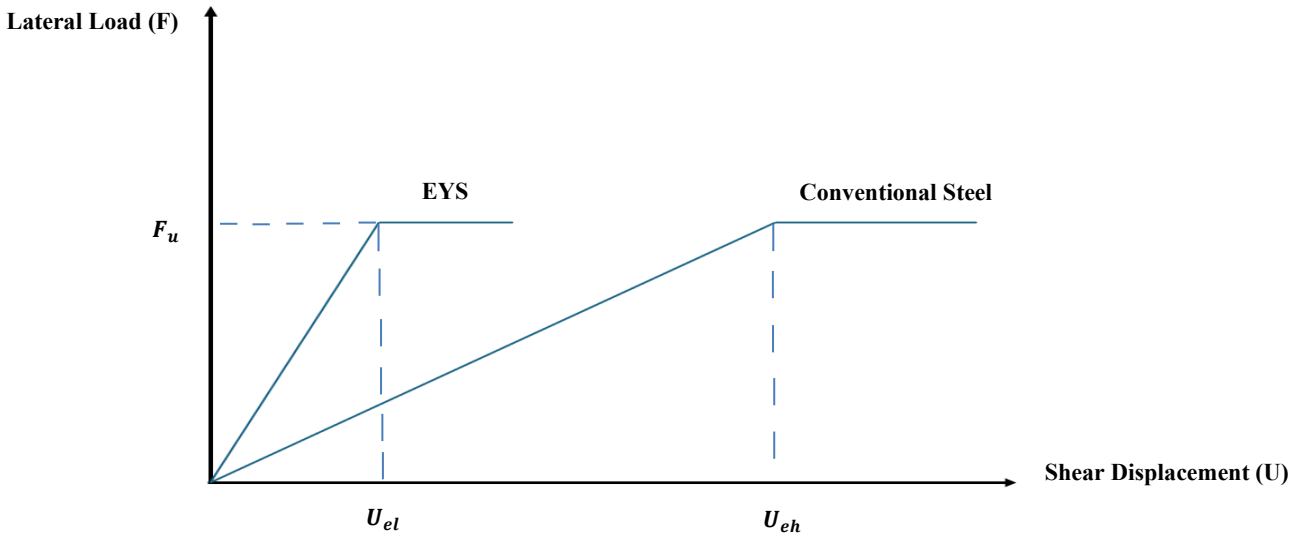

Fig. 2: Comparison of shear displacement versus lateral load for EYS and conventional structural steels

When the EYS is employed for the plates of the same width, in order to achieve a steel plate with the same ultimate strength as conventional structural steel, the procedure outlined in Equation (1) must be followed [2]. In Equation (1), the subscript 1 is used for parameters related to conventional structural steel, while the subscript 2 denotes parameters related to EYS.

$$F_{wu1} = F_{wu2} \rightarrow \frac{1}{2} L t_1 \sigma_{0_1} = \frac{1}{2} L t_2 \sigma_{0_2} \rightarrow \quad t_2 = \frac{\sigma_{0_1}}{\sigma_{0_2}} t_1 \tag{1}$$

In Equation (1), F_{wu} represents the ultimate strength of the steel plate, t denotes the plate thickness, and σ_0 indicates the yield stress of the steel plate. L represents the span width of the steel plate shear wall. Since the yield stress of conventional structural steel (σ_{0_1}) is higher than that of EYS (σ_{0_2}), the ratio $\frac{\sigma_{0_1}}{\sigma_{0_2}}$ is greater than one. Consequently, the thickness of the EYS plate (t_2) must be greater than that of the conventional steel plate (t_1). This increase in thickness, as indicated in Equation (2), leads to a reduction in the story shear displacement of the steel plate shear wall.

$$U_w = \frac{4F}{E} \times \frac{H}{Lt} \tag{2}$$

In Equation (2), the parameter U_w represents the story shear displacement, which depends on the lateral force of F, the story height of H, and the modulus of elasticity of the steel (E). According to Equation (3), the ratio of story shear displacements obtained using EYS to those obtained using conventional structural steel, is equal to the reciprocal of their plate thicknesses.

$$\frac{U_{w_2}}{U_{w_1}} = \frac{\frac{4F}{E} \times \frac{H}{Lt_2}}{\frac{4F}{E} \times \frac{H}{Lt_1}} = \frac{t_1}{t_2} \tag{3}$$

Therefore, since t_2 is greater than t_1 according to Equation (1), U_{w_2} is smaller than U_{w_1}. Furthermore, according to Equation (4), when using EYS plates, the critical stress, such as the plate buckling limit, increases proportionally to the square of the thickness ratio [2].

$$\frac{\tau_{cr2}}{\tau_{cr1}} = \frac{\frac{K\pi^2 E}{12(1-\mu^2)}(\frac{t_2}{L})^2}{\frac{K\pi^2 E}{12(1-\mu^2)}(\frac{t_1}{L})^2} \rightarrow \quad \frac{\tau_{cr2}}{\tau_{cr1}} = (\frac{t_2}{t_1})^2 \tag{4}$$

In Equation (4), the parameters τ_{cr} and μ represent the critical stress, such as the plate buckling limit, and the Poisson's ratio of the steel plate, respectively. It should be noted that, similar to the modulus of elasticity, the Poisson's ratio of EYS is the same as that of conventional structural steel. Furthermore, according to Equation (5), the critical load corresponding to the plate buckling increases proportionally to the cube of the thickness ratio [2].

$$\frac{F_{wcr_2}}{F_{wcr_1}} = \frac{Lt_2\tau_{cr2}}{Lt_1\tau_{cr1}} = \frac{t_2}{t_1} \times \frac{\tau_{cr_2}}{\tau_{cr_1}} = \frac{t_2}{t_1} \times \left(\frac{t_2}{t_1}\right)^2 \rightarrow \frac{F_{wcr_2}}{F_{wcr_1}} = (\frac{t_2}{t_1})^3 \tag{5}$$

In Equation (5), the parameter F_{wcr} represents the critical load corresponding to the plate buckling. It should be noted that in Equation (5), the relationship derived from Equation (4) was also employed, and the ratio of the critical buckling stresses of the plates was replaced by the square of the thickness ratio.

It has been observed that the use of EYS plates reduces the shear displacement, thereby increasing the story shear stiffness. These advantages not only protect the primary vertical structural members of the building but also mitigates the adverse effects of the P-Δ phenomenon on the structure. Additionally, the use of EYS plates allows the plate to enter the inelastic range under relatively small lateral displacements, enabling it to absorb the majority of the energy. This ensures that other structural members remain within the elastic range, preventing damage. When EYS plates are employed, the critical stress, such as the buckling limit, increases, which leads to greater energy absorption by the plate and, consequently, an improvement in hysteretic behavior**.**

4. Specimen Design

This study is conducted on a one-story, prototype-scale numerical model. As previously mentioned, the Plate–Frame Interaction Method is employed for the specimen design. Before addressing the design procedure of the specimen, the underlying design assumptions are described.

4.1. Design Assumptions

1. The steel used in the plates is an EYS with these properties: yield stress σ_0=100 MPa; thickness t =2 mm; modulus of elasticity E = 210 GPa; and Poisson's ratio μ=0.3. However, the steel used in the frame is the conventional structural steel (ST37).
2. IVBEs have smaller cross-sections compared to EVBEs and are generally considered secondary columns. However, IVBEs must be sufficiently strong to ensure the formation of the Diagonal Tension Field (DTF) across the entire steel plate.
3. HBEs and CBs have identical cross-sections, and a continuous beam is used in practice, though with different flange and web thicknesses.
4. Energy dissipation must first occur in the steel plate, followed by the participation of the surrounding frame.
5. IVBEs are discontinuous and are terminated at the beam–column connection level.
6. The specimen investigated in this study is a one-story, prototype-scale numerical model, extracted from a multi-story building.
7. To simulate the load transferred from the plates in the upper stories onto the specimen, stronger sections are considered for the HBEs, ensuring that these beams remain within the elastic range and do not enter the inelastic domain.
8. The span widths of the two shear panels are assumed to be equal.
9. Gravitational loads are neglected in the analysis and design.

10. Considering the thinness of the steel plate, simplified formulations for thin steel plates, as presented in reference [1], are adopted.

4.2. Design Procedure

Before presenting the design procedure, it is necessary to introduce the notations used throughout this study due to their frequent use:

- M_{fp}: Plastic moment capacity
- M_y: Yield moment capacity
- S. F: Shape factor
- σ_{ty}: Yield stress of the Diagonal Tension Field (DTF)
- σ_y: Yield stress of the steel frame
- σ_0: Yield stress of the steel plate
- t: Thickness of the steel plate
- H: Height of the shear panel
- h: Section depth of the members
- I_f: Moment of inertia of the members (about the strong axis)
- S_{zz}: Elastic section modulus of the members (about the strong axis)
- $S_{zz,P}$: Plastic section modulus of the members (about the strong axis)
- U_{we}: Yield displacement of the steel plate
- U_{fe}: Yield displacement of the steel frame

At the beginning of the design procedure, based on assumption 2 (formation of a diagonal tension field across the entire steel plate), a lower bound for the plastic section modulus of the interior columns (IVBE) is obtained. According to the relation presented in [1], to ensure the formation of the diagonal tension field in the entire steel plate, inequality of (6) must be satisfied.

$$(M_{fp})_{IVBE} > \frac{\sigma_{ty} t H^2}{16} \tag{6}$$

After substituting the parameter of M_{fp} with its equivalent expression, and replacing σ_{ty} with σ_0 (due to the thinness of the plate), inequality (7) is obtained.

$$\begin{aligned} &(S.F)_{IVBE} \times (M_y)_{IVBE} > \frac{\sigma_0 t H^2}{16} \rightarrow \\ &(S.F)_{IVBE} \times \frac{2(I_f)_{IVBE}}{h_{IVBE}} \times \sigma_y > \frac{\sigma_0 t H^2}{16} \rightarrow \\ &(S.F)_{IVBE} \times (S_{zz})_{IVBE} \times \sigma_y > \frac{\sigma_0 t H^2}{16} \rightarrow \\ &(S_{zz,P})_{IVBE} \times \sigma_y > \frac{\sigma_0 t H^2}{16} \rightarrow \\ &(S_{zz,P})_{IVBE} > \frac{\sigma_0 t H^2}{16\sigma_y} \end{aligned} \tag{7}$$

In the next step, considering the assumption 4 (energy dissipation occurring first in the plate), the steel plate must yield prior to internal and external columns. To achieve this, based on the relationships provided in [1], inequalities (8) and (9) must be satisfied.

$$U_{we} < (U_{fe})_{IVBE} \tag{8}$$

$$U_{we} < (U_{fe})_{EVBE} \tag{9}$$

Furthermore, according to [1], equations (10) and (11) are used to calculate the yield displacements of the internal and external columns.

$$(U_{fe})_{IVBE} = \frac{(M_{fp})_{IVBE} H^2}{6E(I_f)_{IVBE}} \tag{10}$$

$$(U_{fe})_{EVBE} = \frac{(M_{fp})_{EVBE} H^2}{6E(I_f)_{EVBE}} \tag{11}$$

By substituting the equivalent plastic moment parameters into relations (10) and (11), equations (12) and (13) are obtained.

$$\begin{aligned} (U_{fe})_{IVBE} &= \frac{(S.F)_{IVBE} \times \frac{2(I_f)_{IVBE}}{h_{IVBE}} \times \sigma_y H^2}{6E(I_f)_{IVBE}} \rightarrow \\ (U_{fe})_{IVBE} &= \frac{(S.F)_{IVBE} \times \sigma_y H^2}{3E h_{IVBE}} \end{aligned} \tag{12}$$

$$\begin{aligned} (U_{fe})_{EVBE} &= \frac{(S.F)_{EVBE} \times \frac{2(I_f)_{EVBE}}{h_{EVBE}} \times \sigma_y H^2}{6E(I_f)_{EVBE}} \rightarrow \\ (U_{fe})_{EVBE} &= \frac{(S.F)_{EVBE} \times \sigma_y H^2}{3E h_{EVBE}} \end{aligned} \tag{13}$$

Furthermore, reference [1] provides a relation for calculating the yield displacement of the steel plate (U_{we}), which is presented in Equation (14).

$$U_{we} = \frac{2\sigma_0 H}{E} \tag{14}$$

By substituting equations (12) to (14) into equations (8) and (9), equations (15) and (16) are obtained.

$$\begin{aligned} &\frac{2\sigma_0 H}{E} < \frac{(S.F)_{IVBE} \times \sigma_y H^2}{3E h_{IVBE}} \rightarrow \\ &h_{IVBE} < \frac{(S.F)_{IVBE} \times \sigma_y H}{6\sigma_0} \end{aligned} \tag{15}$$

$$\begin{aligned} &\frac{2\sigma_0 H}{E} < \frac{(S.F)_{EVBE} \times \sigma_y H^2}{3E h_{EVBE}} \rightarrow \\ &h_{EVBE} < \frac{(S.F)_{EVBE} \times \sigma_y H}{6\sigma_0} \end{aligned} \tag{16}$$

Thus, Equations (15) and (16) provide an upper bound for the section heights of the internal and external columns. For the continuation of the design, it is crucial to ensure that the yielding sequence of the members follows the designer's expectation and logical reasoning. The intended yielding sequence in this study is as follows:

1. Steel Plates: Because they are easily replaceable and prevent damage to the frame members.
2. External Vertical Boundary Elements (EVBEs): Because these members, after the steel plates, play

the most significant role in energy dissipation, and among the frame members; after HBEs, which are not intended to yield, they are the strongest elements.

3. Internal Vertical Boundary Elements (IVBEs): Because these members have the least contribution to energy dissipation and are the weakest structural elements in the coupled steel shear wall system.
4. Horizontal Boundary Elements (HBEs): As mentioned, they should remain within the elastic range.

One of the objectives of this research is also to compare the behavior of coupling beams under shear, intermediate, and flexural yielding. Therefore, the link coupling sections must be selected in such a way that yielding occurs in them during seismic loading using nonlinear static (pushover) analysis. Figure 3 summarizes the expected yielding sequence.

* HBEs should not yield and CBs should yield.

Fig. 3: Designer's intended yielding sequence in this study

Thus, the specimen is designed using Equations (7), (15), (16) and the sections of the main beams (HBEs) and coupling beams (CBs) are selected in such a way that yielding does **not** occur in the HBEs but **does** occur in the CBs. This has been achieved through a trial-and-error process by considering various section properties in the Abaqus software. According to Assumption 6, this study is conducted on a prototype- scale numerical specimen. Therefore, the height of the shear panel should be approximately 3 meters. In this study, the shear panel height is considered exactly as H=3000 mm. Accordingly, based on the known values in Equations (7), (15), and (16), these relations are rewritten as presented in Equations (17) to (19).

$$\begin{aligned}&\left(S_{zz,P}\right)_{IVBE}\\&> \frac{100\ \left(N/mm^2\right) \times 2(mm) \times 3000^2(mm^2)}{16 \times 240\ \left(N/mm^2\right)}\\&\rightarrow (S_{zz,P})_{IVBE} > 468750\ mm^3\end{aligned} \tag{17}$$

$$\begin{aligned}&h_{IVBE}\\&< \frac{(S.F)_{IVBE} \times 240\ \left(N/mm^2\right) \times 3000\ (mm)}{6 \times 100\ \left(N/mm^2\right)}\\&\rightarrow\\&h_{IVBE} < 1200 \times (S.F)_{IVBE}\ \ (mm)\end{aligned} \tag{18}$$

$$\begin{aligned}&h_{EVBE}\\&< \frac{(S.F)_{EVBE} \times 240\ \left(N/mm^2\right) \times 3000\ (mm)}{6 \times 100\ \left(N/mm^2\right)}\\&\rightarrow\\&h_{EVBE} < 1200 \times (S.F)_{EVBE}\ \ (mm)\end{aligned} \tag{19}$$

Therefore, the final design relations are those presented in Equations (17) to (19) and it is again emphasized that the HBE and CB sections are determined through a trial-and-error approach in Abaqus, such that yielding occurs in the CBs but not in the HBEs. Numerous sections satisfy the design criteria given in Equations (17) to (19); however, in this study, the sections illustrated in Figure 4 are employed.

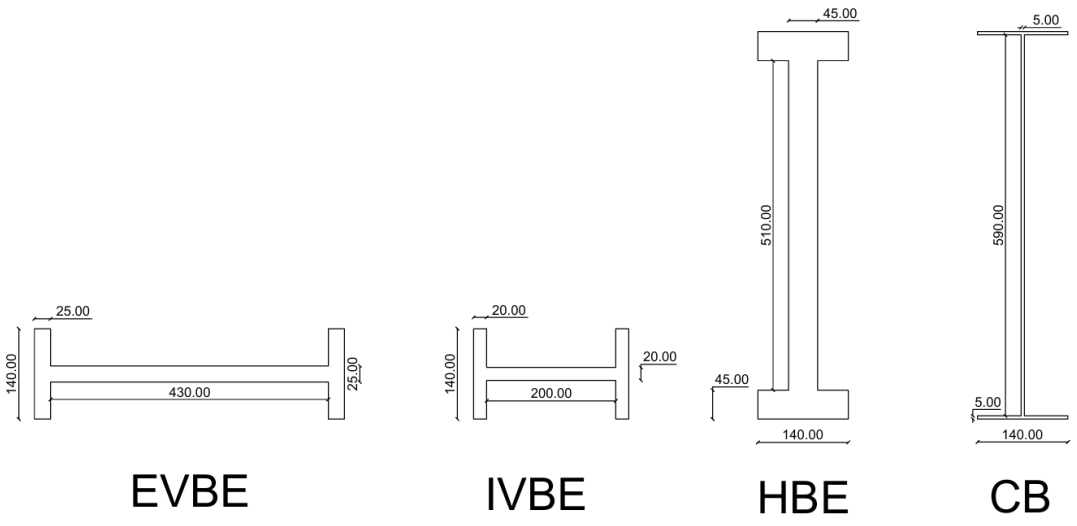

Fig. 4: Designed sections of this study

Finally, some other important points regarding the design are noted:

1. As mentioned, there is no unique solution for the design; any set of sections that satisfies Equations (17) to (19) constitutes a valid design solution. Furthermore, the designed section for the main beams (HBE) must be sufficiently strong to prevent

yielding, and the designed sections for CBs must be adequately weak to ensure yielding.
2. For the beam-to-column connections, the flange width of the beams must be less than or equal to the flange width of the columns. In this study, all flange widths are considered equal to 140 mm.
3. The verification of the provided sections is performed using Abaqus, with special attention paid to the yielding sequence.
4. The geometric parameter of the span width for each shear panel is set to L=3000 mm, and the geometric parameter of the coupling beam length (e) is discussed later.

5. Determination of the Behavioral Range of Coupling Beams

One of the influential parameters in this study is the length of the coupling beam (CB). If the length of the beam is below a certain threshold, its yielding mechanism is predominantly shear-dominated, whereas if it exceeds a certain limit, the yielding mechanism is predominantly flexure-dominated. Within a specific range, the beam exhibits a combined behavior.

Several relations have been proposed to determine the performance range of various types of beams, including coupling beams. In this study, the relations presented by Kasai and Popov in [25], which are considered highly accurate, are employed. Before presenting these relations, the notations used are listed again.

- e: Length of the coupling beam
- M_p: Plastic moment of the coupling beam section
- V_p: Plastic shear of the coupling beam section
- σ_y: Yield stress of the used steel in coupling beam section
- d: Overall depth of the coupling beam section
- b_f: Flange width of the coupling beam section
- t_f: Flange thickness of the coupling beam section
- t_w: Web thickness of the coupling beam section

According to the relations presented in [25], the lengths e_1 and e_2 must first be calculated using equations (20) and (21).

$$e_1 = 1.6 \times \frac{M_p}{V_p} \tag{20}$$

$$e_2 = 2.6 \times \frac{M_p}{V_p} \tag{21}$$

According to Reference [25], coupling beams with a length shorter than e_1 exhibits the **shear-dominant behavior**, while those with a length greater than e_2 exhibits the **flexural-dominant behavior**. Beams with lengths between e_1 and e_2 demonstrate a **combined shear–flexural behavior**. Reference [25] has also provided equations (22) and (23) for calculating M_p and V_p, respectively.

$$M_p = \sigma_y t_f (d - t_f)(b_f - t_w) \tag{22}$$

$$V_p = \frac{\sigma_y t_w (d - t_f)}{\sqrt{3}} \tag{23}$$

For the section shown for the CB in Figure 4, which satisfies the yielding condition, the values of M_p and V_p have been calculated using equations (24) and (25).

$$M_p = 240\,{}^{N}/_{mm^2} \times 5mm \times (600 - 5)mm \times (140 - 5)mm = 9.639 \times 10^7\ N.mm \tag{24}$$

$$V_p = \frac{240\,{}^{N}/_{mm^2} \times 5mm \times (600 - 5)mm}{\sqrt{3}} = 412228.0922\ N \tag{25}$$

By substituting the obtained values of M_p and V_p from equations (24) and (25) into equations (20) and (21), the performance ranges for the coupling beam shown in Figure 3 are determined. These values are presented in equations (26) and (27).

$$e_1 = 1.6 \times \frac{9.639 \times 10^7\ N.mm}{412228.0922\ N} = 374.12\ mm \tag{26}$$

$$e_2 = 2.6 \times \frac{9.639 \times 10^7\ N.mm}{412228.0922\ N} = 607.95\ mm \tag{27}$$

Therefore, according to equations (26) and (27), if the considered coupling beam has a length, approximately of less than **374 mm**, it predominantly exhibits the **shear behavior**, while if its length exceeds approximately **608 mm**, it predominantly exhibits the **flexural behavior**. In this study, a length of **e = 300 mm** was assigned to the coupling beam specimen with shear-dominated behavior, and **e = 2000 mm** was assigned to the specimen with flexure-dominated behavior. Also, a length of **e = 500 mm**, was considered for the specimen exhibiting **combined shear–flexural behavior**.

Regarding the coupling beams considered in this study, two additional important points should be noted. First, since the specimens are modeled at prototype-scale, a question may arise as to whether the selected coupling beam lengths are too short. In response, it should be mentioned that the openings created in coupled steel plate shear wall systems are typically provided for architectural, not structural, purposes. Therefore, these openings do not necessarily need to be as large as a typical doorway that allows the passage of a person of normal size. Since this research focuses purely on structural behavior, it is assumed that the openings considered here are intended for windows or utility passages.

Second, unlike the sections designed for HBE, EVBE, and IVBE, the section adopted for the coupling beam is not seismically compact. However, such a section has been used for two main reasons:

1. If larger sections satisfying seismic compactness requirements were used, the yielding condition for the coupling beams would not be met, which would contradict one of the primary design objectives.
2. The use of stiffeners in the coupling beam section significantly prevents local buckling and mitigates other potential issues arising from the non-compactness of the section under seismic loading.

Finally, it should be noted that the nature of this research is numerical rather than experimental; therefore, less emphasis has been placed on factors that might cause difficulties in practical implementation.

Figures 5 to 7 respectively illustrate the overall configuration of the specimens with shear, combined, and flexural coupling beam behavior. As shown in these figures, stiffeners have been used in all structural members as required and positioned appropriately.

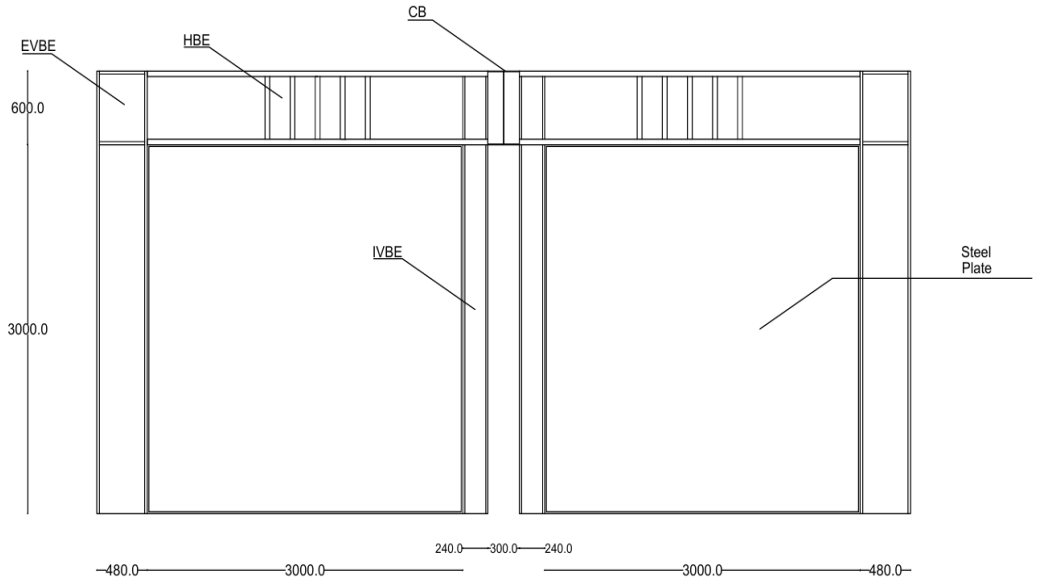

Fig. 5: Overall configuration of the specimen with shear-dominated coupling beam behavior

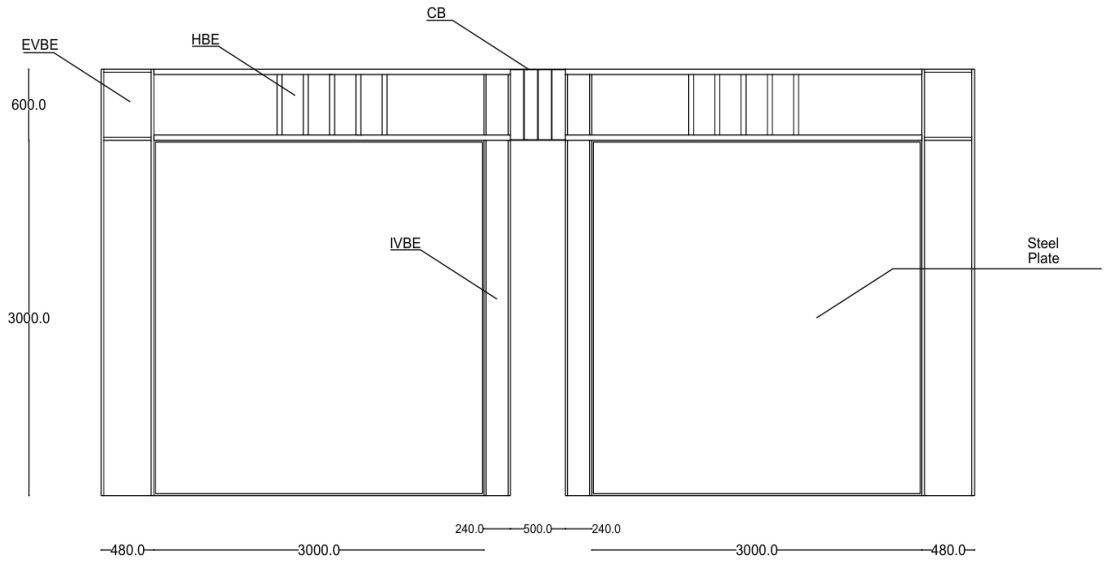

Fig. 6: Overall configuration of the specimen with combined shear-flexural coupling beam behavior

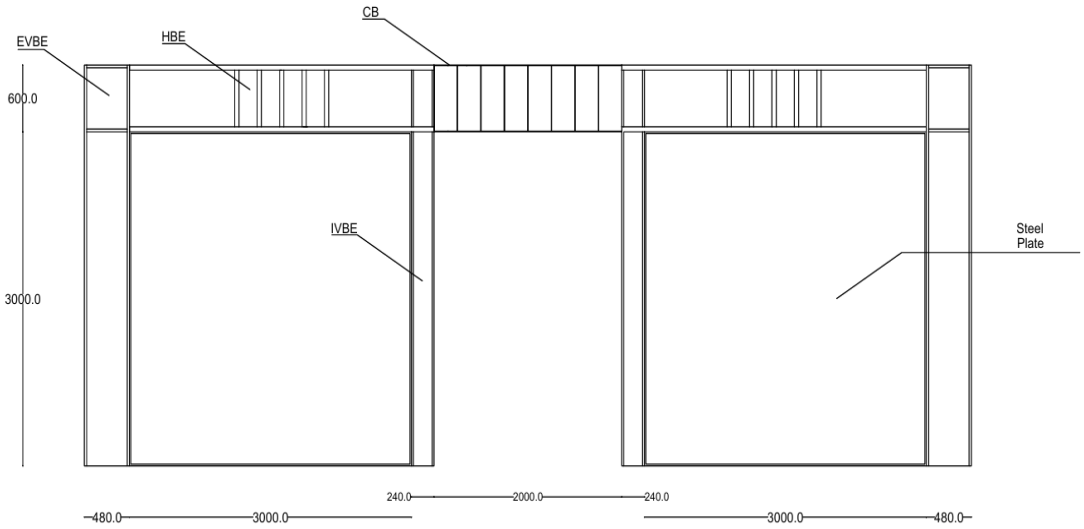

Fig. 7: Overall configuration of the specimen with flexure-dominated coupling beam behavior

In the following, these three specimens with different behaviors are modeled in the finite element software, *Abaqus* and subjected to nonlinear static (pushover) analysis in order to investigate their various seismic parameters.

6. Numerical Investigation in Abaqus

In this section, the three models presented in the previous part are modeled using the finite element software, *Abaqus* and the main results, including the yielding sequence as well as the pushover curve under nonlinear static analysis, are examined. The results are then presented and analyzed separately. All structural components of the coupled steel plate shear wall system, including infill plates, coupling beams, boundary beams, columns, and stiffeners, were modeled using shell elements. This modeling approach is justified by the thin-walled nature of the members, where the thickness of plates and steel sections is small compared to their in-plane dimensions, and the structural response is primarily governed by membrane and bending actions. For such systems, shell elements are well established to accurately capture global stiffness, yielding sequence, load–displacement behavior, and energy dissipation characteristics. Previous numerical and experimental studies have shown that, provided an adequate mesh density is employed, shell-based models yield global responses that are in close agreement with those obtained from solid element modeling, while offering significantly improved computational efficiency. Since the objective of this study is to evaluate the overall performance limits and dominant the behavioral modes (shear, flexural, and combined) rather than local through-thickness stress concentrations, the use of shell elements is considered both appropriate and sufficient. To ensure the accuracy and reliability of the numerical simulations, a mesh sensitivity analysis was conducted to determine the optimal mesh size. Different mesh densities were evaluated by systematically refining the mesh until key output parameters (e.g., stress, displacement, etc.) showed negligible variation with further refinement. This approach guarantees a balance between computational efficiency and solution accuracy, minimizing discretization errors while avoiding unnecessarily fine meshes. The selected mesh size corresponds to the point where results converge within an acceptable tolerance, ensuring that the simulation outcomes are independent of mesh resolution. The effects of nonlinear geometric deformations were considered in finite element analysis of the specimens.

In order to enhance the modeling accuracy in *Abaqus*, the following considerations have been applied to all models:

1- All column-to-base connections have been assumed to be **fixed**, and this condition has been modeled consistently in all models.

2- To ensure the presence of **lateral supporting** in the developed models, the **out-of-plane displacements** of all beams and columns have been **restrained.**

3- To account for **fabrication imperfections** in the steel plates, an **out-of-plane displacement of 5 mm** has been applied to the center of these plates.

4- For conducting the **nonlinear static (Pushover) analysis**, a **maximum lateral displacement** must be applied to both ends of the specimens. In this study, a **drift ratio of 4%** has been considered for all models. Although such a drift is significantly higher than what typically occurs under normal conditions, it was adopted in order to observe the **yielding sequence of all frame members** after the yielding of the infill plates. Given that the height of the studied panels is **H = 3000 mm**, the corresponding applied lateral displacement equals **4% of this height**, i.e., **120 mm**, which has been implemented in all models.

6.1. Shear Model

As discussed, the shear-dominated model has a relatively shorter link beam, and according to the relationships presented in reference [25], the link beam's length of this model was set to e = 300 mm. Subsequently, the yield sequence of the various components of the coupled steel plate shear wall system with a shear-dominated link beam was examined in Abaqus. The results confirmed the expected sequence mentioned earlier in Figure 3, which was also observed in the software and is presented in Figures 8 to 12.

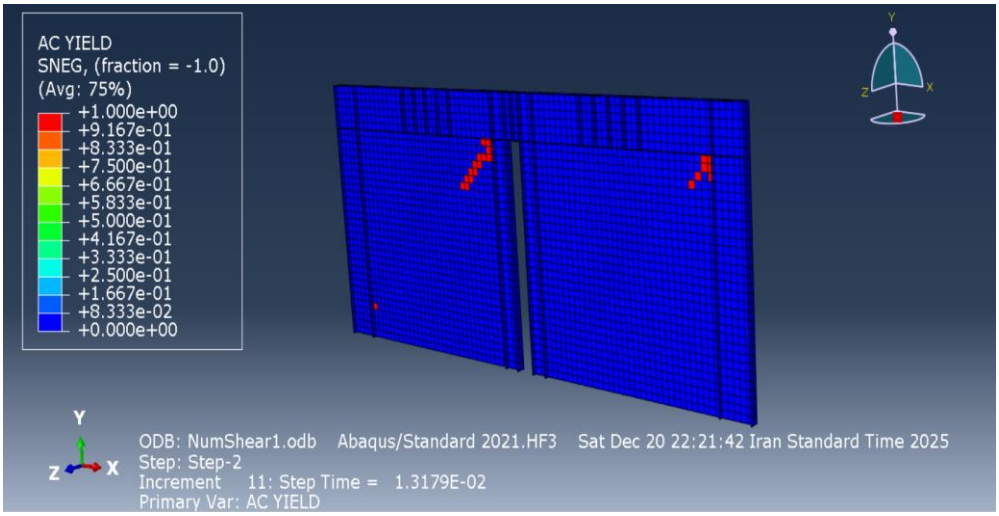

Fig. 8: First yielding observed in the steel plates of the shear-dominant specimen with a yield stress of 100 MPa, occurring at time step 11

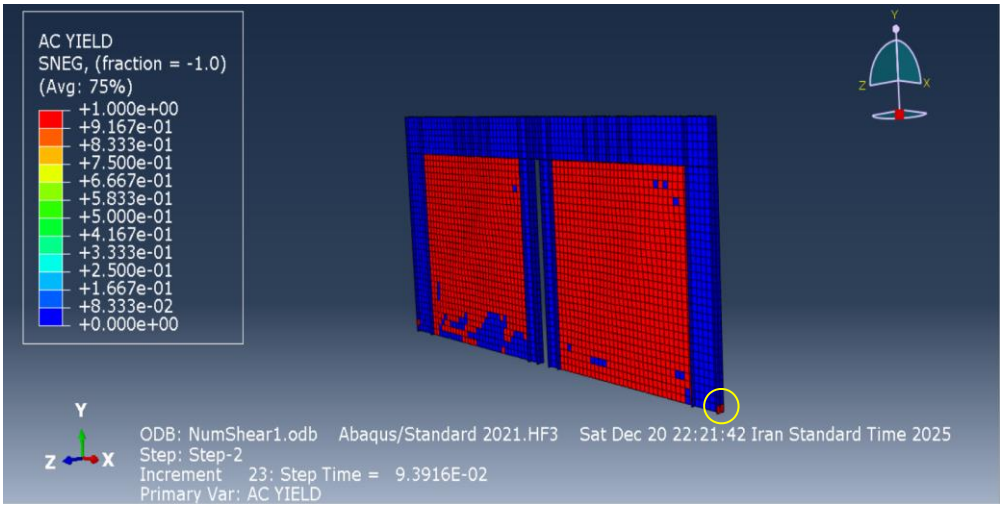

Fig. 9: Second yielding observed in the bottom end of EVBEs of the shear-dominant specimen with a yield stress of 240 MPa, occurring at time step 23

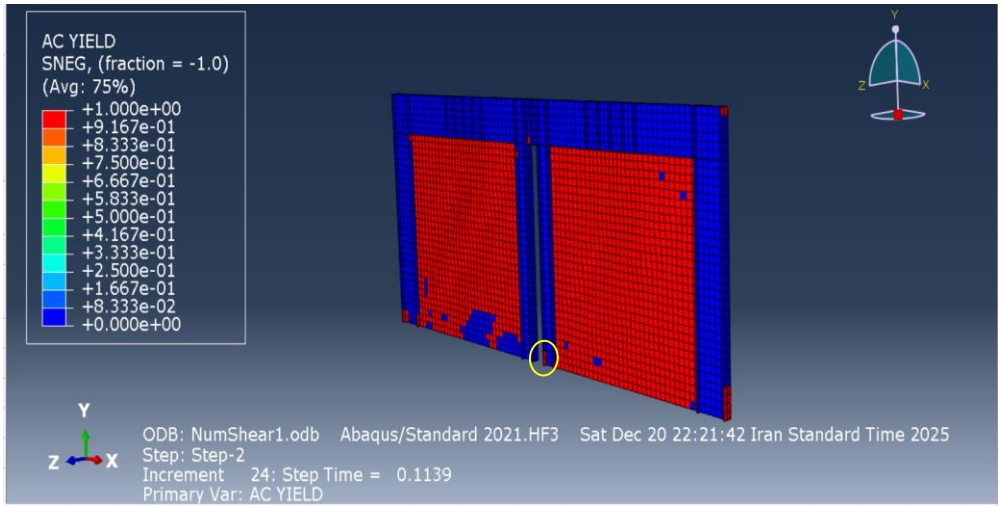

Fig. 10: Third yielding observed in the bottom end of IVBEs of the shear-dominant specimen with a yield stress of 240 MPa, occurring at time step 24

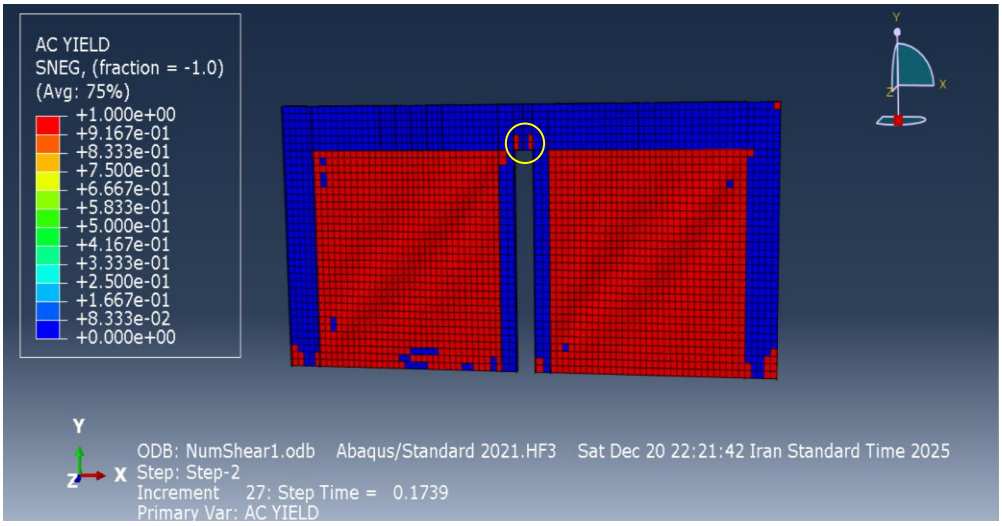

Fig. 11: Fourth yielding observed in the web of CB of the shear-dominant specimen with a yield stress of 240 MPa, occurring at time step 27

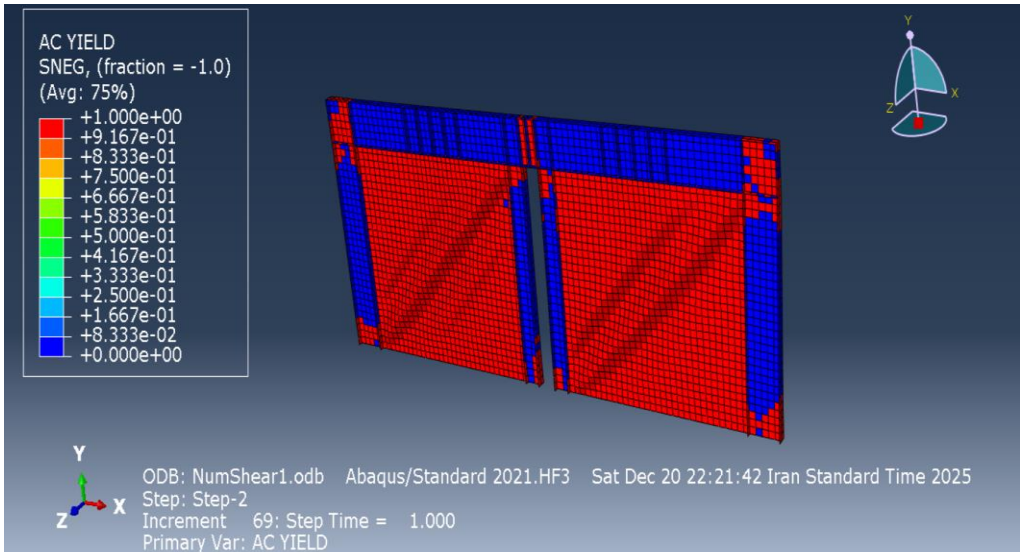

Fig. 12: Final loading step in the shear-dominant model (step 69) with no yielding in HBEs

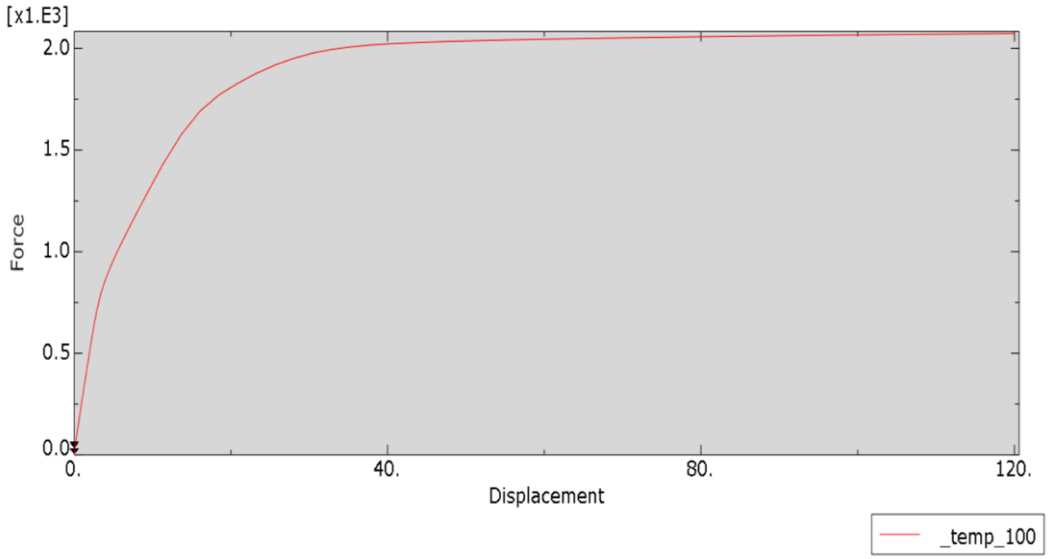

Fig. 13: Pushover curve of the coupled steel shear wall specimen with a shear-dominated coupling beam (force in kgf and displacement in mm).

As can be seen in Figure 12, yielding has occurred in all members except the HBEs, and therefore the objective of keeping the HBEs from yielding has also been achieved.
Finally, the pushover curve obtained from the Abaqus software for the shear-dominated model after completing the nonlinear static analysis is presented below in Figure 13. The inflection points of the curve indicate the yielding of different components of the coupled steel shear wall system. As shown in the figure, the ultimate load of the specimen with shear-dominated link behavior is 207.36 tonf.
By exaggerating the vertical displacement of the coupling beam specimen with predominantly shear behavior, it is observed that the beam exhibits the **expected shear-dominated response** both in terms of **yielding mode** and **deformation pattern**, which confirms the high accuracy of the behavioral ranges presented in Reference [25]. In shear yielding, plastic hinges form at both ends while the **web fully yields**. Moreover, the vertical deformation of the shear-dominated specimen is **sharp and without any curvature**, and both of these characteristics are clearly visible in Figure 14.

6.2. Combined Shear-Flexural Model

As discussed, the combined shear-flexural model has a medium coupling beam in terms of length, and according to the relationships presented in [25], the coupling beam's length of this model was set to e = 500 mm. Subsequently, the yield sequence of the various components of the coupled steel plate shear wall system with a combined shear-flexural link beam was examined in Abaqus. The results confirmed the expected sequence mentioned earlier in Figure 3, which was also observed in the software and is presented in Figures 15 to 19.

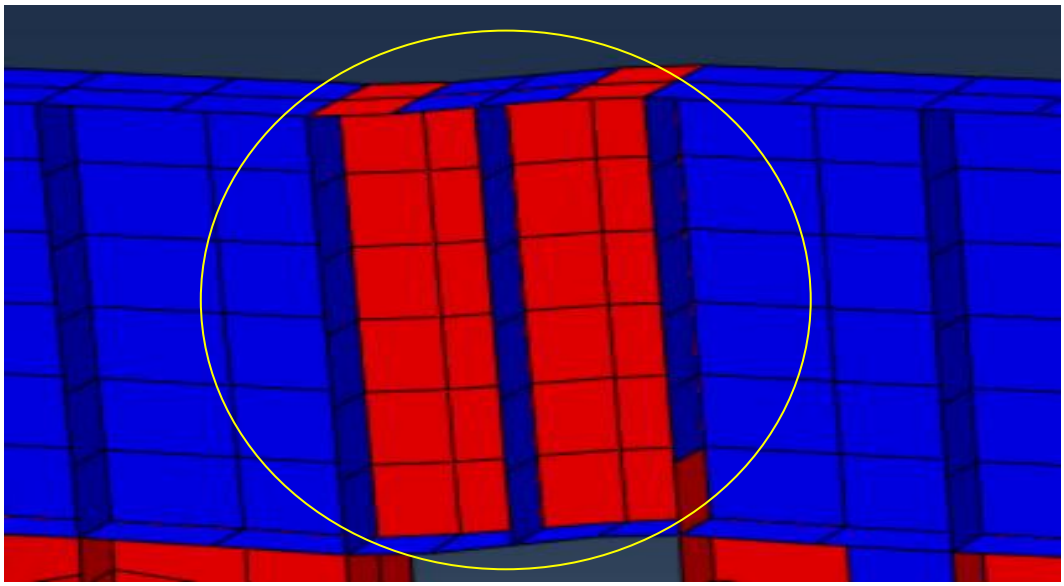

Fig. 14: Demonstration of Shear Behavior of the Link Beam by exaggeration of vertical deformations in the last step of loading (time step 69)

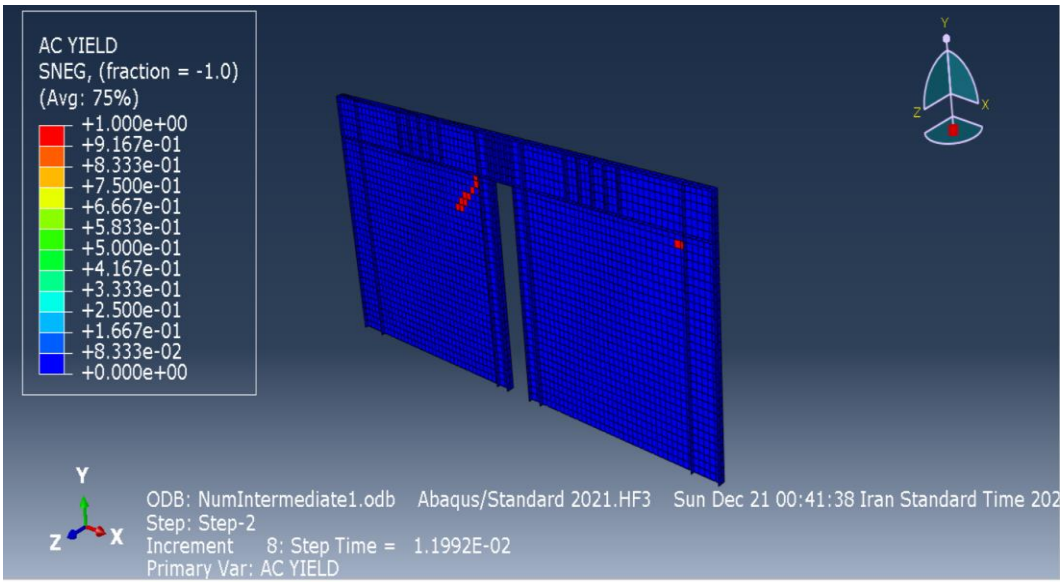

Fig. 15: First yielding observed in the steel plates of the combined shear-flexural specimen with a yield stress of 100 MPa, occurring at time step 8

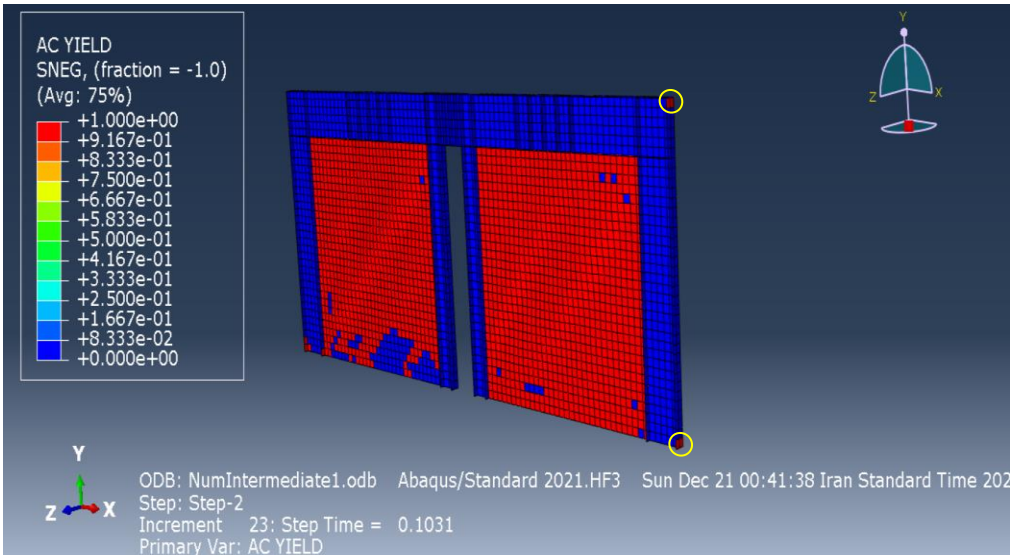

Fig. 16: Second yielding observed in the top and bottom ends of EVBEs of the combined shear-flexural specimen with a yield stress of 240 MPa, occurring at time step 23

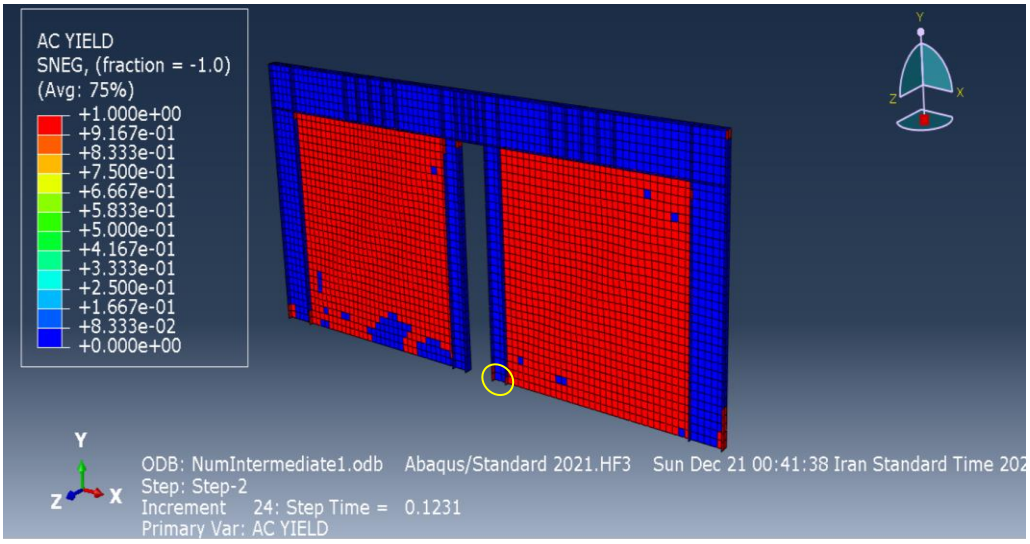

Fig. 17: Third yielding observed in the bottom end of IVBEs of the combined shear-flexural specimen with a yield stress of 240 MPa, occurring at time step 24

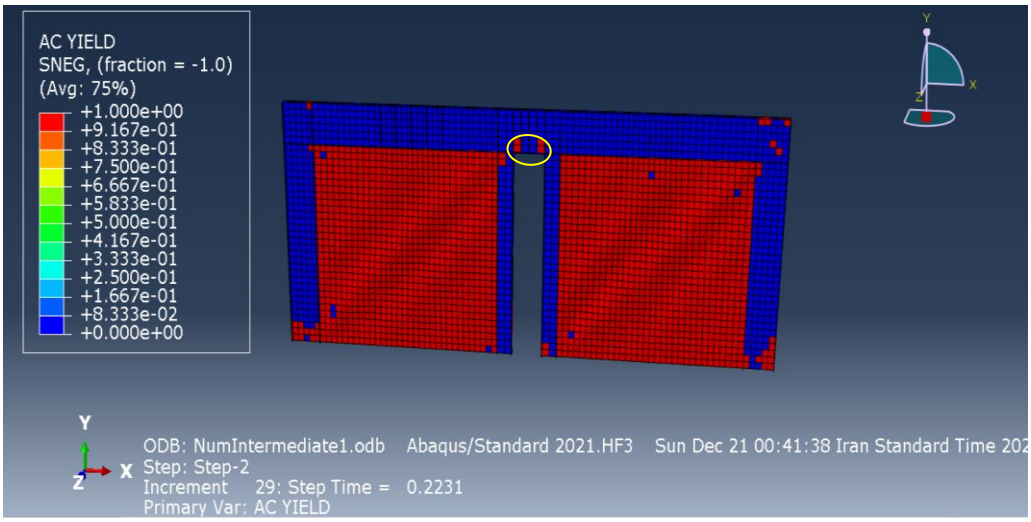

Fig. 18: Fourth yielding observed in the CB's web of the combined shear-flexural specimen with a yield stress of 240 MPa, occurring at time step 29

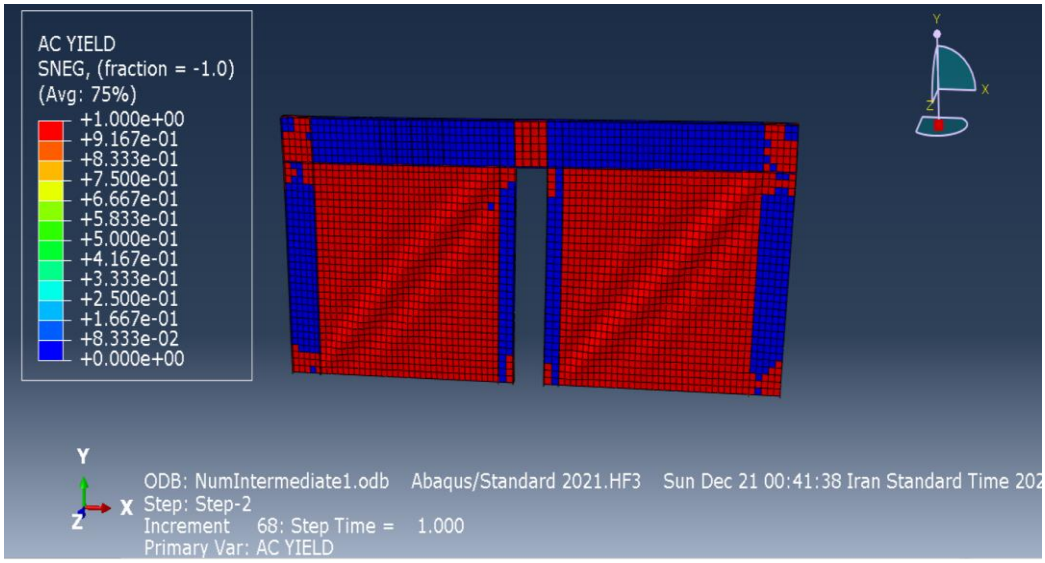

Fig. 19: Final loading step in the shear-flexural model (step 68) with no yielding in HBEs

As can be seen in Figure 19, yielding has occurred in all members except the HBEs, and therefore the objective of keeping the HBEs from yielding has also been achieved. Finally, the pushover curve obtained from the Abaqus software for the combined shear-flexural model after completing the nonlinear static analysis is presented below in Figure 20. The inflection points of the curve indicate the yielding of different components of the coupled steel shear wall system. As shown in the figure, the ultimate load of the specimen with combined shear-flexural link behavior is 207.41 tonf.

By exaggerating the vertical displacement of the coupling beam specimen with **combined behavior**, it is observed that the beam exhibits the **expected yielding and deformation pattern**, further confirming the high accuracy of the behavioral ranges provided in Reference [25]. In combined yielding, plastic hinges form at both ends while the **web undergoes yielding.** Moreover, the vertical deformation of the combined-behavior specimen is **sharp and exhibits slight curvature**, both of these characteristics are clearly evident in Figure 21.

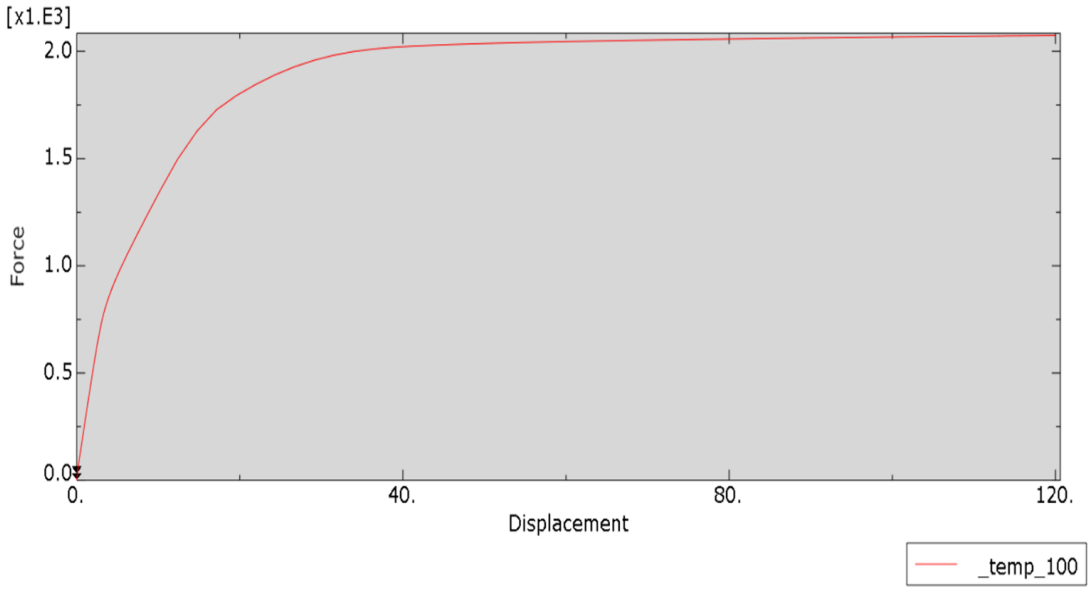

Fig. 20: Pushover curve of the coupled steel shear wall specimen with a combined shear-flexural coupling beam (force in kgf and displacement in mm).

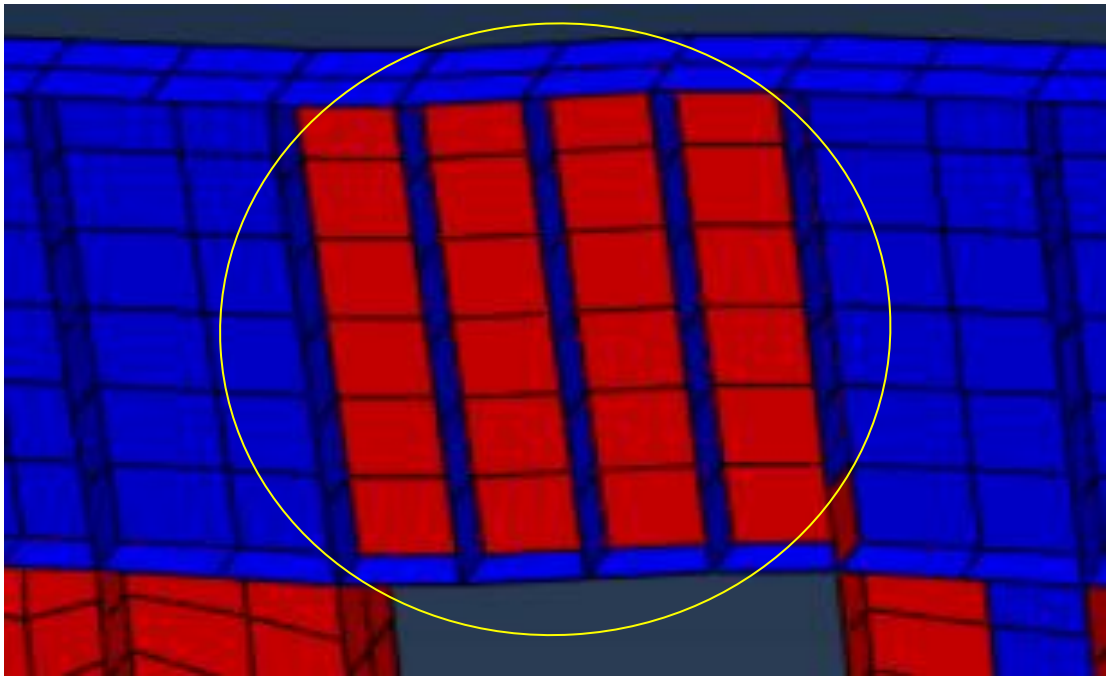

Fig. 21: Demonstration of combined shear-flexural behavior of the coupling beam by exaggeration of vertical deformations in the last step of loading (time step 67)

6.3. Flexural Model

As discussed, the flexural model has a relatively longer link beam, and according to the relationships presented in [25], the link beam's length of this model was set to e = 700 mm. Subsequently, the yield sequence of the various components of the coupled steel plate shear wall system with a flexural link beam was examined in Abaqus. The results confirmed the expected sequence mentioned earlier in Figure 3, which was also observed in the software and is presented in Figures 22 to 26.

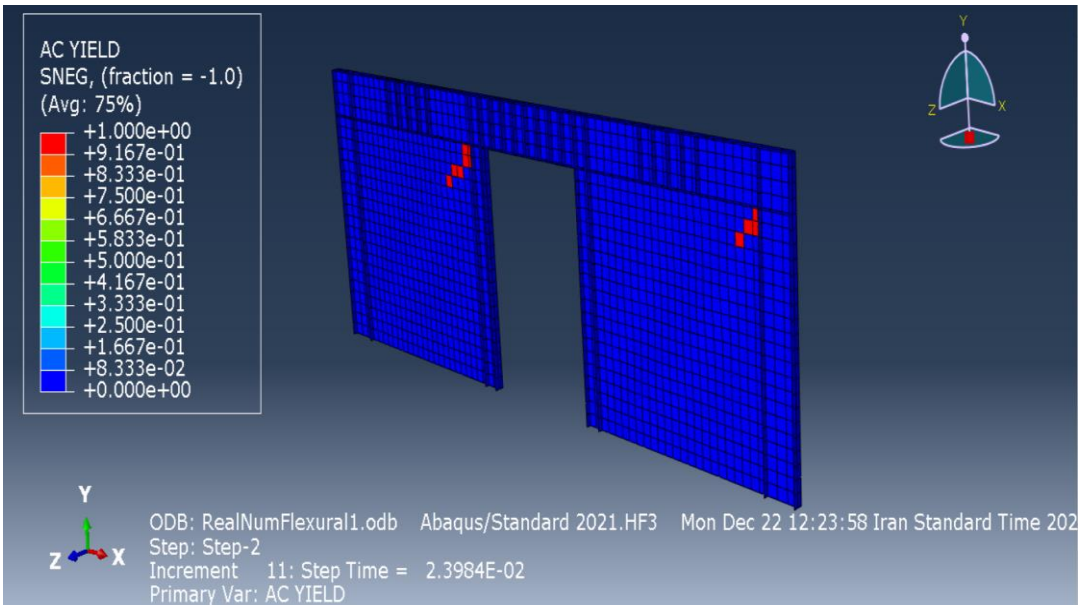

Fig. 22: First yielding observed in the steel plates of the flexural-dominant specimen with a yield stress of 100 MPa, occurring at time step 11

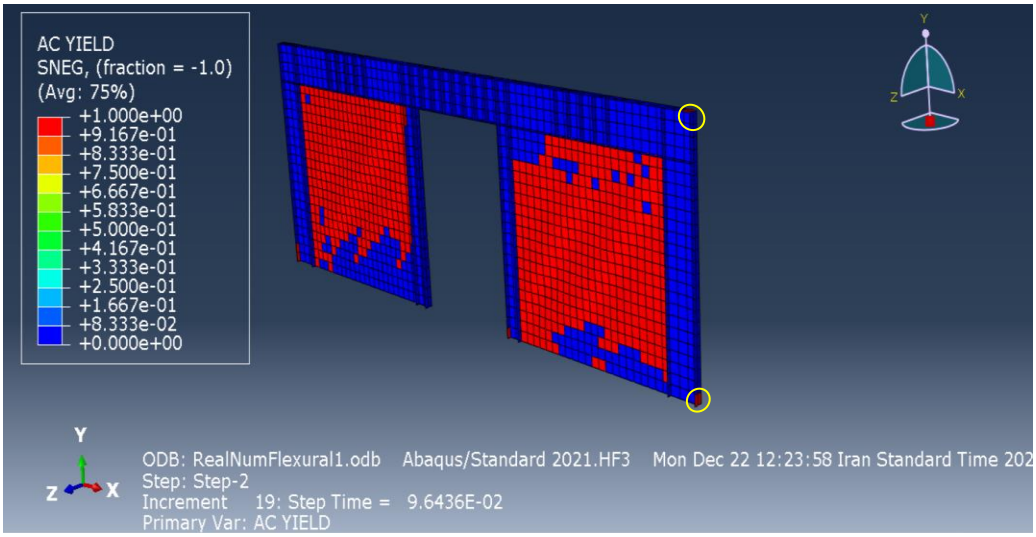

Fig. 23: Second yielding observed in the top and bottom ends of EVBEs of the flexural-dominant specimen with a yield stress of 240 MPa, occurring at time step 19

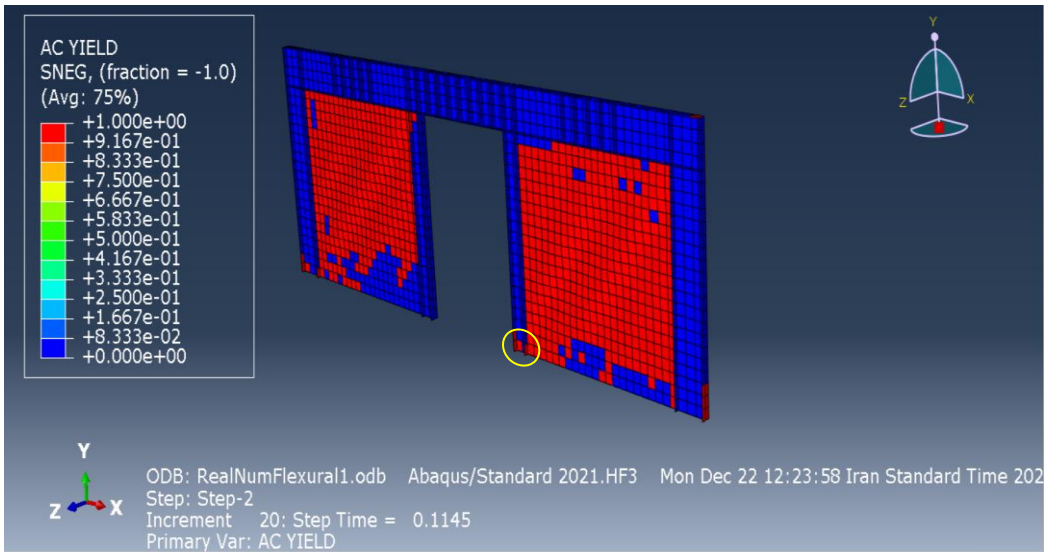

Fig. 24: Third yielding observed in the bottom ends of IVBEs of the flexural-dominant specimen with a yield stress of 240 MPa, occurring at time step 20

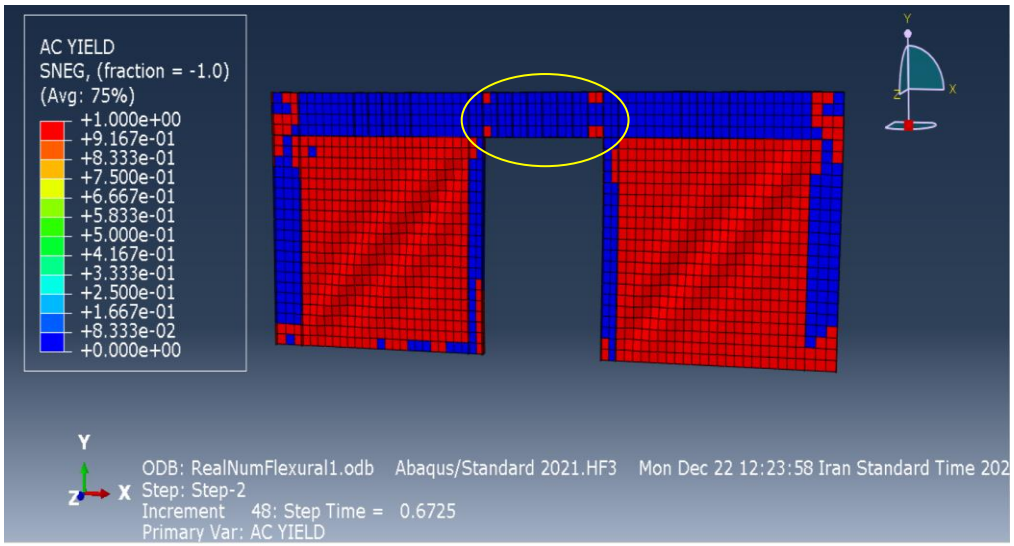

Fig. 25: Fourth yielding observed in the web of CB of the flexural-dominant specimen with a yield stress of 240 MPa, occurring at time step 48

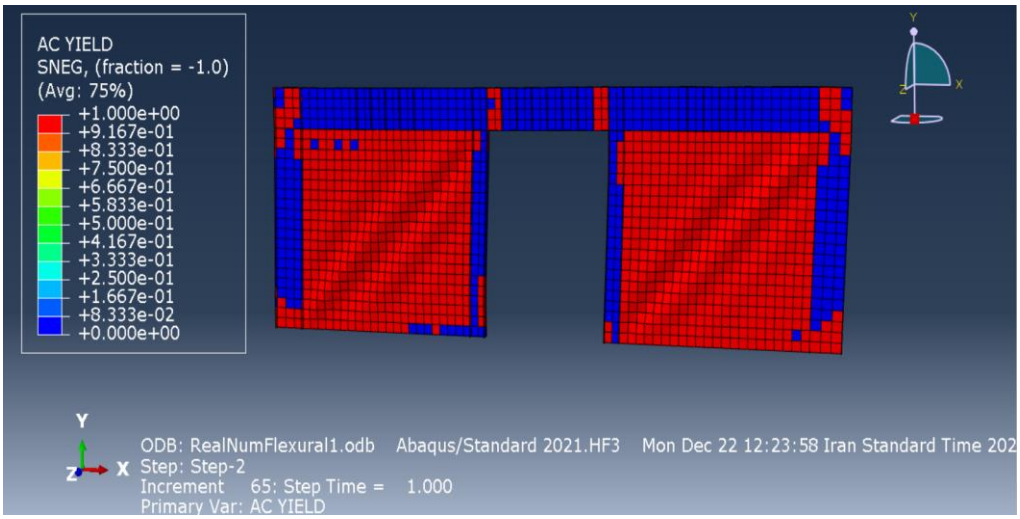

Fig. 26: Final loading step in the flexural-dominant model (step 65) with no yielding in HBEs

As can be seen in Figure 26, yielding has occurred in all members except the HBEs, and therefore the objective of keeping the HBEs from yielding has also been achieved. Finally, the pushover curve obtained from the Abaqus software for the flexural model after completing the nonlinear static analysis is presented below in Figure 27. The inflection points of the curve indicate the yielding of different components of the coupled steel shear wall system. As shown in the figure, the ultimate load of the specimen with flexural-dominated coupling beam behavior is 210.26 tonf.

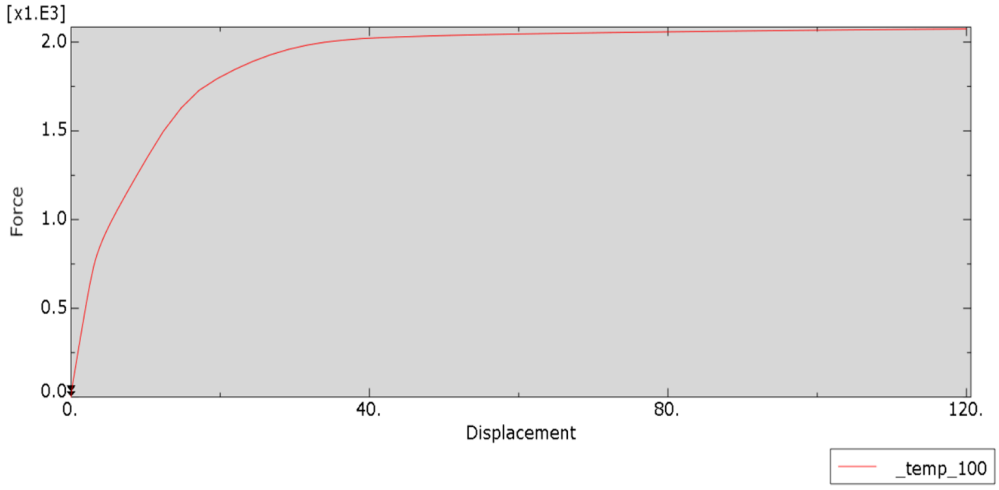

Fig. 27: Pushover curve of the coupled steel shear wall specimen with a flexural-dominant link beam (force in kgf and displacement in mm).

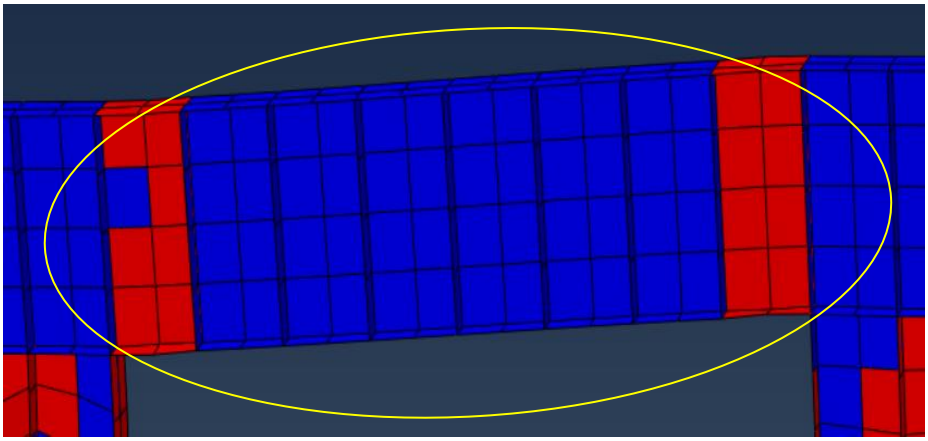

Fig. 28: Demonstration of flexural behavior of the coupling beam by exaggeration of vertical deformations in the last step of loading (time step 65)

By exaggerating the vertical displacement of the coupling beam specimen with **flexural behavior**, it is observed that the beam exhibits the **expected flexure-dominated yielding mode and deformation pattern**, confirming the high accuracy of the behavioral ranges presented in Reference [25]. In flexural yielding, **plastic hinges form only at the two ends**. Additionally, the vertical deformation of the flexural specimen clearly exhibits a **noticeable curvature**, and both of these characteristics are fully evident in Figure 28.

7. Conclusions

In this study, a comprehensive analytical–numerical investigation was conducted on three prototype-scale numerical models of coupled steel plate shear wall specimens with Easy-Yielding steel (EYS) infill plates, exhibiting shear, combined, and flexural behaviors. In general, the findings of this research can be summarized as follows:

1- The use of EYS **plates** leads to a significant improvement in structural properties such as **ductility, energy dissipation,** and overall seismic performance. This improvement was clearly observed in the *Abaqus* simulations of the specimens employing such plates demonstrating that the infill plates act as the primary energy dissipating components while protecting the surrounding frame members from excessive inelastic deformations.

2- The **coupled steel plate shear wall system** is one of the most efficient seismic load-resisting systems, because not only it offering an excellent structural performance in various aspects, the presence of an opening between the walls also provides significant **architectural flexibility and advantages.**

3- By using the **plate–frame interaction (PFI) design method**, the designer can accurately impose the desired **yielding sequence** on the system. In practice, the steel infill plate acts as the **first and primary source of energy dissipation**, and even at drift levels far beyond typical limits, it prevents the frame members from contributing to energy absorption. This characteristic represents the **most significant advantage** of employing the steel plate shear wall system.

4- The behavioral ranges demonstrated by the specimens were observed to perform with a high level of accuracy. The use of flexure-dominated coupling beams clearly allows for larger openings in the structure, which provides a significant architectural advantage. In addition, the results of the present study, based on pushover analyses, indicate that flexure-dominated specimens provide a greater load-carrying capacity and higher energy dissipation compared to shear-dominated or combined specimens. However, since cyclic degradation effects were not considered in this research, these structural advantages cannot be asserted with certainty and require further investigation in future studies. This observation is particularly relevant given that real buildings often feature large openings that naturally tend to induce flexural behavior in the beams.

References

[1] Sabouri-Ghomi, S. (2002). Lateral load resisting systems: An introduction to steel shear walls. *Angize Pop.*

[2] Sabouri-Ghomi, S. (2004). Lateral Load Resisting Systems: An Innovative Idea to Application of Easy-going Steel (EGS). *Anguizeh Publishing Company*

[3] Zhao, Q., & Astaneh-Asl, A. (2004). Cyclic behavior of traditional and innovative composite shear walls. *Journal of Structural Engineering, 130(2)*, 271-284.

[4] Choi, I. R., & Park, H. G. (2009). Steel plate shear walls with various infill plate designs. *Journal of structural engineering, 135(7),* 785-796.

[5] Borello, D. J., & Fahnestock, L. A. (2012). Behavior and mechanisms of steel plate shear walls with coupling. *Journal of Constructional Steel Research, 74,* 8-16.

[6] Abdollahzadeh, G., & Malekzadeh, H. (2013). Response modification factor of coupled steel shear walls. *Civil Engineering Infrastructures Journal, 46(1),* 15-26.

[7] Ahn, T. S., Kim, Y. J., & Kim, S. D. (2013). Large-scale testing of coupled shear wall structures with damping devices. *Advances in Structural Engineering, 16(11),* 1943-1955.

[8] Borello, D. J., Quinonez, A. A., & Fahnestock, L. A. (2014). Steel plate shear walls with coupling in high-seismic regions. In Proc., 10th US National Conf. on Earthquake Engineering: *Frontiers of Earthquake Engineering, NCEE 2014.*

[9] Sadeghi Eshkevari, S., Dolatshahi, K. M., & Mofid, M. (2017). Optimized design procedure for coupling panels in steel plate shear walls. *The Structural Design of Tall and Special Buildings, 26(1),* e1301.

[10] Pavir, A., & Shekastehband, B. (2017). Hysteretic behavior of coupled steel plate shear walls. *Journal of Constructional Steel Research, 133,* 19-35.

[11] Gorji, M. S., & Cheng, J. R. (2018). Plastic analysis and performance-based design of coupled steel plate shear walls. *Engineering Structures, 166,* 472-484.

[12] Shayanfar, M., Broujerdian, V., & Ghamari, A. (2020). Analysis of coupled steel plate shear walls with outrigger system for tall buildings. *Iranian Journal of Science and Technology, Transactions of Civil Engineering, 44(1),* 151-163.

[13] Usefvand, M., Maleki, A., & Alinejad, B. (2020). Investigate of damage index of coupled steel plate shear walls (C-SPSW) system under seismic loading. In *Structures (Vol. 28, pp. 614-625).* Elsevier

[14] Wang et. Al (2021). Damage indices and fragility assessment of coupled low-yield-point steel plate shear walls. *Journal of Building Engineering, Volume 42,103010, ISSN 2352-7102.*

[15] Hao, J., Li, S., Tian, W., & Wu, X. (2023). Seismic performance of coupled steel plate shear wall with slits. *Journal of Constructional Steel Research*, 195, 107480.

[16] Zirakian, T. (2024). Methodical investigations on seismic retrofitting of steel plate shear wall systems using low-yield-point steel. *Buildings*, 14(1), 258.

[17] Seismic performance evaluation of hybrid coupled shear wall system with shear and flexural fuse-type steel coupling beams (2024). *Computer Modeling in Engineering & Sciences*, 135(2), 1205-1230.
[18] Experimental studies on seismic and replaceable behaviors of hybrid coupled walls with a low-yield-point steel shear panel damper (2025). *Structures*, 52, 1028-1045.
[19] Pehlivan, B. M., Baran, E., & Topkaya, C. (2025). Seismic behavior of cold-formed steel framed multi-panel and two-story shear walls. *Bulletin of Earthquake Engineering*, 23(2), 1575-1596.
[20] Alhunami, H., El-Gohary, H. A., & Bazuhair, R. W. (2025). Evaluation of the dynamic characteristics of coupled shear wall systems under seismic loads. *Engineering, Technology & Applied Science Research*, 15(1), 10411-10422.
[21] Assessment of the seismic performance of prefabricated coupling beam connections (2024). *Buildings*, 15(23), 4387.
[22] Seismic performance enhancement of shear wall structures using lead viscoelastic coupling beams (2025). *Engineering Structures*, 335, 116054.
[23] Modeling and seismic performance analysis of grid shear walls (2025). *Buildings*, 15(2), 294.
[24] Experimental investigation on the seismic performance of novel prefabricated composite RC shear walls with CFST frame (2024). *Buildings*, 14(10), 2930.
[25] Kasai, K., & Popov, E. P. (1986). General behavior of WF steel shear link beams. *Journal of Structural Engineering*, *112*(2), 362-382.